

## Collective transitions at high level density

G. Leander\*

*Florida State University, Tallahassee, Florida**and UNISOR, Oak Ridge Associated Universities, Oak Ridge, Tennessee 37830*

(Received 30 October 1981)

It has been assumed that highly excited collective bands, more or less parallel to the yrast line, are important for the gamma deexcitation of rotational nuclei formed in heavy-ion reactions. This paper draws attention to the possibility that the in-band decay of any given state may be spread over a broad spectrum and discusses the implications for the cascade process. A simple model, where bands are generated by coherent matrix motion in the Gaussian orthogonal ensemble, indicates how the spreading width may depend on the fundamental nature of nuclear level structure.

[ NUCLEAR STRUCTURE Model for collective bands at high level  
density. Spreading of in-band transitions and consequences for  
quasicontinuum gamma cascades at very high spin. ]

## I. INTRODUCTION

Many reactions populate nuclear states in regions of high level density. Information on the structure of such states has earlier been obtained from the width and spacing of neutron resonances<sup>1</sup> and from the shape of giant resonances.<sup>2</sup> The theoretical many-body approaches that have been developed include statistical distributions in random matrices for the neutron resonances, and single-particle response functions to describe the spreading of the collective strength in giant resonances.

A new situation arises in the gamma deexcitation of nuclei formed at very high spin in heavy-ion fusion reactions. The gamma cascades proceed in up to 30 or 40 small steps, initially through an energy band above the yrast line where the level density at each spin and even close to the yrast line is presumably quite high. Nuclear structure effects can be resolved from the resulting quasicontinuum gamma-ray spectra, and the results indicate that rotational bands often play an important role for the deexcitation process.<sup>3</sup> A fairly good description of the quasicontinuum singles spectrum and side-feeding intensities has been obtained in statistical cascade calculations, where collective transitions approximately parallel to the yrast line are included as an additional decay mode.<sup>3-7</sup> Theoretical descriptions of the many bands involved have assumed that a reasonable model is provided, for example, by the

triaxial rotor model<sup>4</sup> or the cranked deformed shell model.<sup>6</sup> These models are known to be successful at lower spins in the pairing regime where level densities are low.

It does seem plausible that a deformed nucleus can rotate collectively even when heated, provided that the surface diffuseness due to the internal excitations is smaller than the surface deformation. However, the question arises as to how the band structure is affected by the level density,<sup>8,9</sup> One might suspect, by analogy with the giant resonances, that the collectivity is spread over many final states at each step of a cascade, as illustrated schematically in Fig. 1. The transition rate,  $T(E \rightarrow E')$ , is the reduced transition rate,  $B(E \rightarrow E')$ , multiplied by the transition energy to power 5. This  $E_\gamma^5$  dependence favors transitions to the lower tail rather than the peak of the  $B(E \rightarrow E')$  distribution.

A case well known from the study of backbending arises when two bands come close to each other. In general, bands with the same parity but differing by more than one quasiparticle configuration interact through a matrix element,  $V$ , which is small but finite. This interband interaction may inhibit band crossing and keep the  $B(E2)$ 's pointing along the upper branch and the lower branch, respectively. Nevertheless, a cascade which enters the interaction zone on either the upper or the lower branch almost invariably comes out on the *lower*

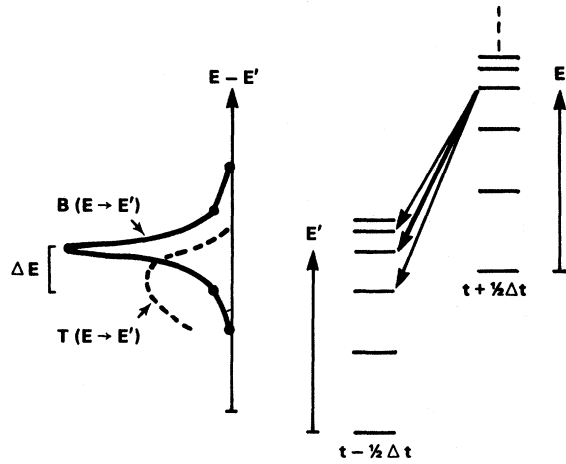


FIG. 1. A schematic illustration of collective transitions over a quantized step  $\Delta t$  in the collective variable  $t$ . The distribution of the collective reduced transition rate over final energies,  $B(E \rightarrow E')$ , is one that was actually calculated, from the  $N=128$  sample described in the text, for an initial energy  $E$  in the middle of the spectrum. The distribution  $T(E \rightarrow E')$  is obtained from  $B(E \rightarrow E')$  by including an energy factor  $(\Delta E_{\text{coll}} + E - E')^5$ , with some arbitrary choice of  $\Delta E_{\text{coll}}$ . The peak of  $T(E \rightarrow E')$  is shifted by an amount  $\Delta E$  from the average in-band value defined by the peak of  $B(E \rightarrow E')$ .

branch due to the energy factor.

It is unclear what happens with many bands at high level density. The next section describes a very simple model based on the random matrix techniques familiar from neutron resonance work, with the addition of a nonperturbative collective degree of freedom that leads to band structure. Like any schematic model, this one cannot resolve the issue but it gives insight into different possibilities and the conditions under which they might be realized. In Secs. III and IV the implications for the nuclear gamma cascade at very high spins are discussed.

## II. THE MODEL

### A. Coherent matrix motion

The Hamiltonian describing collective motion in the variable  $t$ , coupled to intrinsic degrees of freedom, can be written

$$H(i;t) = H_0(i) + H_{\text{int}}(i;t) + H_{\text{coll}}(t), \quad (1)$$

where  $i$  enumerates the intrinsic states,  $H_0$  is the microscopic Hamiltonian in the absence of collective motion,  $H_{\text{coll}}$  describes the macroscopic energy

in terms of  $t$ , and  $H_{\text{int}}$  is the interaction term. Let us now assume that  $H_{\text{int}}$  is linear in  $t$ . This is done, for example, in a simplified version of the cranking Hamiltonian for rotations<sup>10,11</sup>

$$H_c(i;\omega) = H_0(i) - \omega J_x(i) + \frac{1}{2} \mathcal{I} \omega^2, \quad (2)$$

where  $\mathcal{I}$  is the inertial mass,  $\omega$  is the variable canonically conjugate to the cranking coordinate, and  $J_x$  is the corresponding momentum operator in the intrinsic space. Another example is the many-particle plus rotor Hamiltonian

$$H_{pr}(i;I) + H_0(i) - \frac{\hbar^2}{\mathcal{I}} I_1 J_1(i) + \hbar^2 / 2 \mathcal{I} I(I+1), \quad (3)$$

where  $I$  is the total angular momentum. For rotational solutions, the interaction term is approximately linear in  $I$  (e.g., Refs. 10 and 12).

If  $t$  is treated semiclassically, like  $\omega$  of the cranking model, the microscopic degrees of freedom and their coupling to the collective motion can be treated separately from  $H_{\text{coll}}(t)$ . Thereby we avoid having to introduce at least one parameter  $\mathcal{I}$  to characterize  $H_{\text{coll}}$ . The microscopic part of  $H$  is

$$H_\mu(i;t) = H_0(i) + H_{\text{int}}(i;t). \quad (4)$$

Assuming that the intrinsic operators can be restricted to a space of finite dimension  $N$ , the microscopic part  $H_\mu$  of the Hamiltonian becomes a linear combination of two  $N \times N$  matrices  $\hat{A}$  and  $\hat{B}$

$$\hat{H}_\mu = \hat{A} + t\hat{B}. \quad (5)$$

Another parametrization, equivalent for small  $t$ , is

$$\hat{H}_\mu = \sqrt{1-t^2} \hat{A} + t\hat{B}. \quad (6)$$

The square root factor on the truncated intrinsic Hamiltonian  $\hat{A}$  may be taken to represent polarization with increasing  $t$ , corresponding, for example, to a change of the nuclear shape from prolate to oblate with increasing spin. Practically, it conserves normalization in the calculations below. The effect is smooth except for  $t$  close to unity, where the rate of change of the square root diverges.

The lowest eigenstates of  $\hat{H}_\mu$  are shown as a function of  $t$  in Fig. 2, for some arbitrary choice of the matrices  $\hat{A}$  and  $\hat{B}$ . The spectrum of  $\hat{A}$  is obtained at  $t=0$  and the spectrum of  $\hat{B}$  at  $t=1$ . Coherent matrix motion from  $\hat{A}$  to  $\hat{B}$  is obtained by the continuous variation of  $t$  from 0 to 1. This generates a spectrum of bands which are smooth except near  $t=1$  and at a few sharp band crossings. In general one may speak of a band-crossing regime

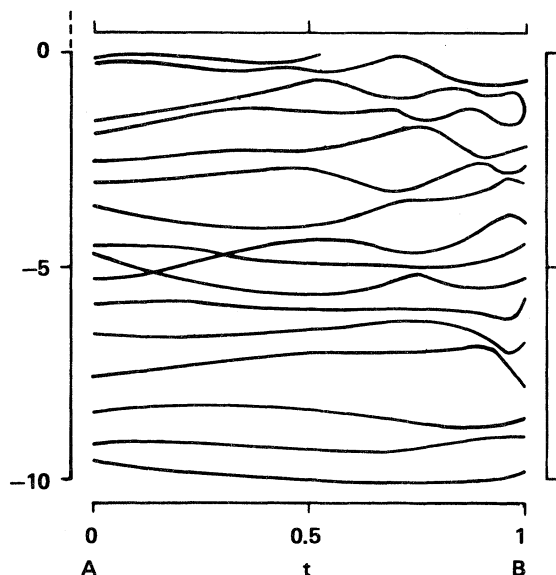


FIG. 2. An example of band structure obtained from the Hamiltonian (6) by continuous variation of  $t$ . Here  $\hat{A}$  and  $\hat{B}$  are two 32-dimensional random matrices from the distribution (7) with  $\epsilon=0$ . Only the lower half of the spectrum is shown.

when the interaction  $V$  between two bands is typically smaller than the mean spacing  $\rho^{-1}$  between the bands. If the magnitude of  $V$  is held constant and the level density  $\rho$  is increased, one would expect to approach the ergodic limit where individual band characteristics such as different slopes are washed out. The case in Fig. 2 is clearly intermediate in this respect, with particularly one distinct up-sloping configuration that goes through a series of sharp band crossings.

Quantization of the collective motion would mean having a spectrum only at discrete values of  $t$  with a spacing  $\Delta t$ , corresponding, for example, to discrete angular momenta. This creates a problem in connecting states at different  $t$  values into bands.

### B. Transitions

In the model used here the collective reduced transition rate,

$$B[E(t + \frac{1}{2}\Delta t) \rightarrow E'(t - \frac{1}{2}\Delta t)],$$

from an initial state at energy  $E$  to a final state at energy  $E'$ , is defined as the square of the overlap of the two eigenvectors, assuming that the same basis

representation is valid at  $t + \frac{1}{2}\Delta t$  and  $t - \frac{1}{2}\Delta t$ . The total collective strength then always adds up to one, corresponding to a state-independent deformation of the rotor in the rotational case, but the strength may be distributed in different ways over the final states. In the band-crossing regime it goes predominantly into one state and that state may be defined as the next state of an intrinsic band. The transition rate defines an "effective" band trajectory, including macroscopic effects from  $H_{\text{coll}}$ , which may or may not favor a different final state. For example, in the two-band case discussed above the transitions to the lower branch win when the energy factor is taken into account.

At higher level density one might generally expect a distribution over several final states. The effective band would consistently lean toward lower final energies than the center of the intrinsic band by some amount  $\Delta E$  (Fig. 1). A realistic absolute estimate of  $\Delta E$  cannot be sought in the present model, however, although it would be easy to introduce an explicit form for  $H_{\text{coll}}$  and to weight the transition rates by  $E_\gamma^5$ . One obvious reason is that the level density in the nucleus is expected to increase rapidly with energy in a way that cannot be simulated with finite matrices. Such variation of the level density over the range of final states would tend to shift the center of the effective band upward and to pinch off the lower tail. Instead, for qualitative purposes, the importance of this effective band behavior will be measured in the calculations by a quantity  $\Delta E$  which is evaluated as the rms deviation of the calculated strength distribution from the centroid using reduced transition rates  $B(E \rightarrow E')$ .

### C. The Gaussian orthogonal ensemble

The matrices  $\hat{A}$  and  $\hat{B}$  of Eq. (6) are taken as random matrices from a Gaussian orthogonal ensemble. The distribution of level spacings obtained from the eigenvalues of such matrices is known to agree with the distribution of spacings observed at high level density in neutron resonance experiments.<sup>1,13</sup> In the following the basic mathematics is reviewed.

A Gaussian orthogonal ensemble is defined in the space of real  $N \times N$  symmetric matrices by the requirement that:

- (1) The ensemble is invariant under every orthogonal transformation, and
- (2) the matrix elements  $M_{ij}$  are statistically independent.

Equivalently, each off-diagonal matrix element has a Gaussian distribution with a constant rms deviation  $V$  from an average of zero, while the diagonal matrix elements are Gaussian with an rms deviation  $\sqrt{2}V$  from an arbitrary average value

$$\begin{aligned} M_{ij} &= N(0, V), \\ M_{ii} &= N(\epsilon, \sqrt{2}V). \end{aligned} \quad (7)$$

The eigenvalues are distributed around the average in the diagonal,  $\epsilon$ . For large  $N$ , the distribution approaches the Wigner semicircle

$$\rho(E) = \frac{1}{2\pi V^2} \sqrt{4NV^2 - (E - \epsilon)^2}. \quad (8)$$

Thus the level density in the interior of the spectrum is of the order of

$$\bar{\rho} = \sqrt{N} / \pi V \quad (9)$$

and drops off sharply at the edges.

It is easily shown that if  $\hat{A}$  and  $\hat{B}$  belong to a Gaussian orthogonal ensemble, then  $\hat{H}_\mu$  defined by Eq. (6) is also a member of the ensemble.

### III. CALCULATIONS AND RESULTS

#### A. Details of the calculations

The parameters of the model are  $\epsilon$ ,  $V$ ,  $N$ ,  $t$ , and  $\Delta t$ . On the technical side, there is also the number of matrix pairs  $(\hat{A}, \hat{B})$  in the statistical sample used to obtain an ensemble average for a given set of parameters. This number has been chosen, depending on  $N$ , so that the total number of eigenstates in each sample is 2560. It is possible to take  $\epsilon=0$  and  $V=1$  without loss of generality. Most of the calculations are done for  $t=0$  and 0.5,  $\Delta t=0.05$ , 0.1, and 0.2.

Samples have been taken for  $N=8$ , 32, and 128. For  $N=128$  only one sample was taken, using  $t=0.5$  and  $\Delta t=0.1$ . The distribution of eigenvalues obtained numerically is plotted in Fig. 3, along with the Wigner semicircles. In each case the semicircle, strictly valid only in the limit of large  $N$ , is seen to describe the numerical distribution quite well. The dashed horizontal line in Fig. 3 shows where the mean level spacing  $\rho^{-1}$  is equal to the rms interaction  $V$  in a random representation. It is seen that for  $N=8$  the mean spacing is larger than the interaction even at maximum level density. For  $N=32$  and 128, on the other hand, the mean level spacing is smaller than  $V$  except for a very few lev-

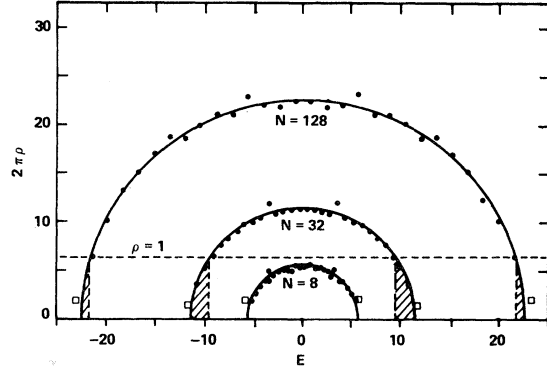


FIG. 3. The Wigner semicircles for  $N=8$ , 32, and 128, and dots representing the distribution of eigenenergies obtained numerically for the matrices  $\hat{B}$  from the samples described in the text. The dots correspond to 30 energy bins, and they are symmetrized around  $E=0$  to improve the statistics. The tails of each distribution are collected into the first and last bins, marked by open squares. Both the eigenenergies  $E$  and the mean level spacing  $\rho^{-1}$  are in units of the variance  $V$  of the interaction matrix elements in a random representation. The entire distribution for  $N=8$ , but only the small shaded parts of the distribution for  $N=32$  and 128, come in the region of  $\rho^{-1} \geq V$  below the horizontal dashed line.

els at the edges, corresponding to the shaded areas. Thus  $N=8$  is in the band-crossing regime, while  $N=128$  is approaching the ergodic regime.

#### B. Fragmentation in the matrix motion model

The quantity  $\Delta E$  defined in Sec. II B above is intended as a measure of how much the transition energies are likely to differ from the in-band value. The calculated relation between  $\Delta E$  and the energy  $E$  of the initial states is shown in Fig. 4. For each  $N$  the range of possible initial energies  $E$ , as given by the diameter of the Wigner semicircle, is divided into 30 bins. The dots in Fig. 4 show  $\Delta E$  in each bin, i.e., evaluated from initial states in the sample which belong to that bin. The horizontal lines in Fig. 4 indicate  $\Delta E$  for a whole sample. Considering the proximity between the dots and the lines in Fig. 4, and noting that the larger statistical fluctuations in the outermost bins arise simply because relatively few initial states lie at the edges of the Wigner semicircle, there is reason to make conjecture 1:  $\Delta E$  is independent of the initial energy  $E$  within a model matrix.

Figure 5 shows the value of  $\Delta E$ , in units of  $V$ , ob-

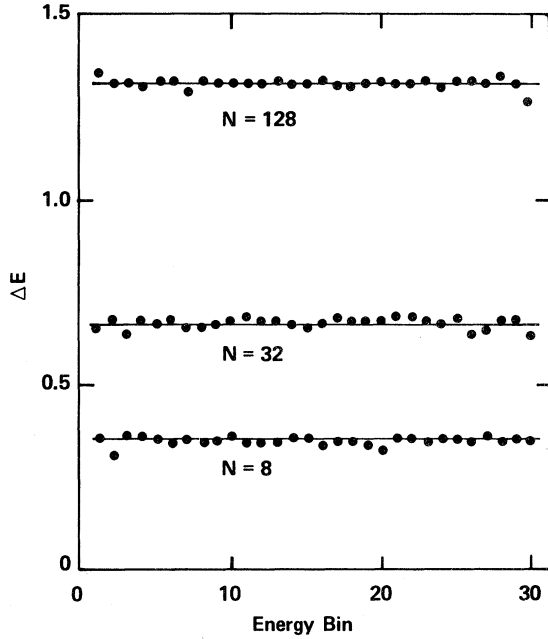


FIG. 4. The broadening  $\Delta E$  of collective transitions, calculated according to the prescription in Sec. II B. Results are shown for three samples with  $N=8$ , 32, and 128, respectively. For each sample  $t=0.5$  and  $\Delta t=0.1$ . The dots show the broadening for different initial energies  $E$ , with the same binning as in Fig. 3. The three lines are for the whole samples.

tained from the whole sample for each of the three samples in Fig. 4 and several others. It is seen that

$$\Delta E \sim k_t \sqrt{N} V \Delta t, \quad (10)$$

where  $k_t$  is approximately equal to 1. It should be mentioned that this dependence on  $t$  and  $\Delta t$  is not a good approximation for small  $\Delta t$  very close to  $t=1$ . An exact result, however, is easily obtained in the special case  $t=0.5$ ,  $\Delta t=1$ . Then a single step connects two independent members,  $\hat{A}$  and  $\hat{B}$ , of the Gaussian orthogonal ensemble and

$$\Delta E = \sqrt{N} V \quad (\Delta t = 1). \quad (11)$$

Equations (9)–(11) suggest conjecture 2:  $\Delta E$  depends on the level density and the interactions through the approximate relation

$$\Delta E \sim \pi \bar{\rho} V^2 \Delta t. \quad (12)$$

It may be noted that a formally similar result has been derived from another schematic model,<sup>14</sup> in which a single extrinsic state is coupled by a constant matrix element to an infinite set of states at constant level density. Then the strength function

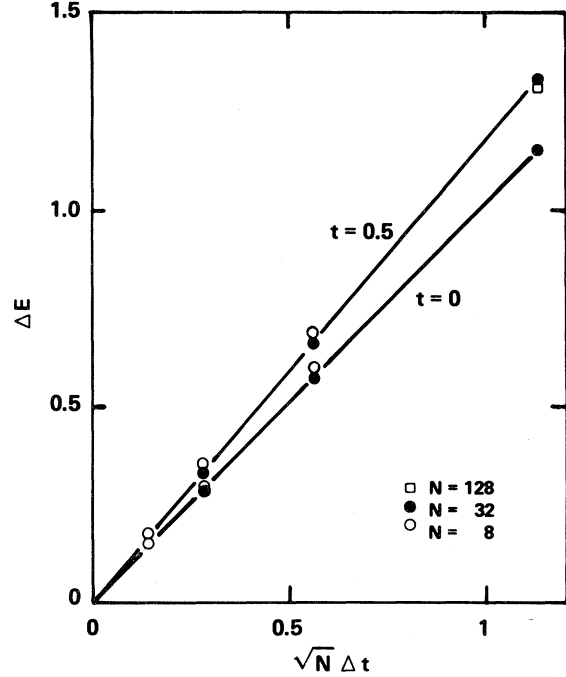


FIG. 5. The broadening  $\Delta E$  of collective transitions, calculated numerically from samples with different values of  $N$ ,  $t$ , and  $\Delta t$ , are plotted versus  $\sqrt{N} \Delta t$ . Straight lines are drawn near the points obtained for  $t=0$  and 0.5, respectively.

can be shown to have the Breit-Wigner form with the width proportional to the level density and the square of the coupling matrix element.

The quantity  $\Delta E$  above measures the deviation in collective cascades from a perfectly smooth trajectory determined by the macroscopic Hamiltonian  $H_{\text{coll}}$ . A different though related quantity of basic interest is the probability that a collective cascade will follow a unique, sharply defined intrinsic band. A qualitative measure of the probability for one sharply in-band transition is the reduced transition rate  $B_{\text{max}}$ , i.e., the square of the largest overlap between the initial state and any one final state. The average value of  $B_{\text{max}}$  obtained from the numerical samples specified above is plotted as a function of  $\Delta E$  in Fig. 6. In the plot  $B_{\text{max}}$  drops smoothly from unity at  $\Delta E=0$  to 0.7 at  $\Delta E \sim 1.3V$  and seems to be bending slightly downward, though asymptotically it must approach zero. This suggests the formulation of conjecture 3: When it is non-negligible the probability for a sharp in-band transition can be estimated as

$$B_{\text{max}} \sim 1 - \Delta E / 4V \sim 1 - \bar{\rho} V \Delta t. \quad (13)$$

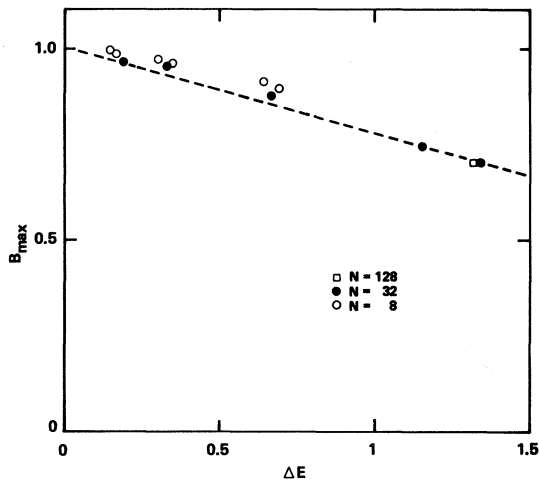


FIG. 6. The average over all initial states of the largest collective reduced transition rate to any individual final state,  $B_{\max}$ , is indicated for each sample as a function of  $\Delta E$ . The dashed line is a linear estimate of the initial decrease in  $B_{\max}$ .

#### IV. DISCUSSION AND CONCLUSIONS

Collective motion is expected to occur in many-body systems even at nonzero temperature, although the coupling to other excited states at similar energy acts to distribute the collective strength over a whole region in excitation energy. A nonperturbative model of band structure at high level density has been studied in this paper. The bands are defined as eigenstate trajectories generated by the continuous and coherent motion of a matrix within the Gaussian orthogonal ensemble. Fragmentation arises when the motion is taken in discrete steps instead, corresponding to quantization. The model clearly has a limited scope and is not intended to simulate a complete physical system. The broadening of the collective transitions is studied in terms of  $\Delta E$ , the rms spread in energy of the initial state vector over the final state vectors, and some general relations have been suggested tentatively on the basis of the results.

These relations have been expressed in terms of the level density,  $\rho$ , and a parameter  $V$ . In the model,  $V$  is the average strength of interactions in the intrinsic space. It scales the effective interactions between eigenstates, i.e., the interactions which give rise to a Wigner-type distribution of level spacings<sup>1,13</sup> and show up as interband interac-

tions when the collective coordinate varies. The collective perturbations are scaled by  $V\Delta t$ . The level density is expected to increase rapidly as a function of the energy above the yrast line, according to a well-known formula based on the number of possible combinations of single-particle states. In an extreme single-particle picture the matrix elements of one-body operators are diluted proportionally to  $\rho^{-1/2}$ , so the spreading width  $\Delta E$  according to Eq. (12) would be independent of the excitation energy above the yrast line. A similar constancy of  $\Delta E$  with respect to excitation energy was found numerically within the random-matrix model space (conjecture 1 above). From the model point of view, it is an interesting question whether the same result would emerge from any finite-matrix approach.

Since the level density varies very rapidly, it is clear from Eq. (12) that the magnitude of  $\Delta E$  depends delicately on the balance between  $\rho$  and  $V^2$ . If there is a residual interaction between different configurations due to some many-body aspect of the nuclear system, so that  $V^2$  decreases more slowly than  $\rho^{-1}$ , the effect could be very large. Let us estimate, for example, what the consequence would be if there is an average residual interaction of 1 keV which does not go away at high level density. Identifying  $t$  with rotational frequency

$$\Delta t = 2\hbar^2 / \mathcal{I} \quad (14)$$

and applying some very crude but adequate estimates for a rotational medium-mass nucleus

$$\begin{aligned} \hbar^2 / 2\mathcal{I} &= 10 \text{ keV} , \\ \rho &= 10^E \text{ MeV}^{-1} , \end{aligned} \quad (15)$$

where  $E$  is the excitation energy above the yrast line in MeV, we have

$$\Delta E = 10^{E-4} \text{ MeV} . \quad (16)$$

Thus the spreading width is 100 keV at 3 MeV above the yrast line, and it increases exponentially at higher energies. In this case collective rotational transitions parallel to the yrast line are important for the gamma cascade at 3 MeV and below, but higher up only small fragments of the collectivity could be playing a role for dominant statistical-like transitions.

In summary, it is possible to conceive three different scenarios for the overall flow of the gamma cascades in rotational nuclei, depending on  $\Delta E$ :

(i)  $\Delta E$  is small at all energies, and the cascades may follow parallel rotational bands as assumed in Refs. 4–7. The line below which collective transitions are predominant slopes upward in energy

versus spin more rapidly than the yrast line and is estimated to reach the entry line at very high spins.<sup>7</sup> On the average, each cascade is expected to follow this collective borderline. [Fig. 7(a).]

(ii)  $\Delta E$  is small below, say, 3 MeV and large above. Effectively, this means that the collective borderline does not rise above 3 MeV even for very high spins.

(iii)  $\Delta E$  is large at all energies. Then all cascades start with a few statistical transitions down into the yrast region, where the major part of the gamma deexcitation takes place [Fig. 7(b)].

It should be possible to test these alternatives experimentally by systematic studies of quasicontinuum spectra. Let us conclude here with some comments on  $\gamma$ - $\gamma$  transition-energy correlation maps, in which a smooth rate of change of the in-band level spacing,  $\Delta^2 E_{\text{coll}}$ , is seen as the separation of two ridges around a central valley.<sup>16</sup> In a medium-mass nucleus,  $\Delta^2 E_{\text{coll}}$  might be about 0.1 MeV. If there are correlations from some region of spin and excitation energy, but they appear on the map as a big blob without ridges and valleys or other structure, it may be inferred that the spreading width is larger than or equal to  $\Delta^2 E_{\text{coll}}$  in this region. Conversely, a smooth ridge-valley structure implies that  $\Delta E$  is smaller than  $\Delta^2 E_{\text{coll}}$ . A bumpy ridge-valley structure may be associated with the region just above yrast where the probability for two consecutive sharply in-band transitions, i.e., the square of  $B_{\text{max}}$  in Eq. (13), is significantly greater than zero.

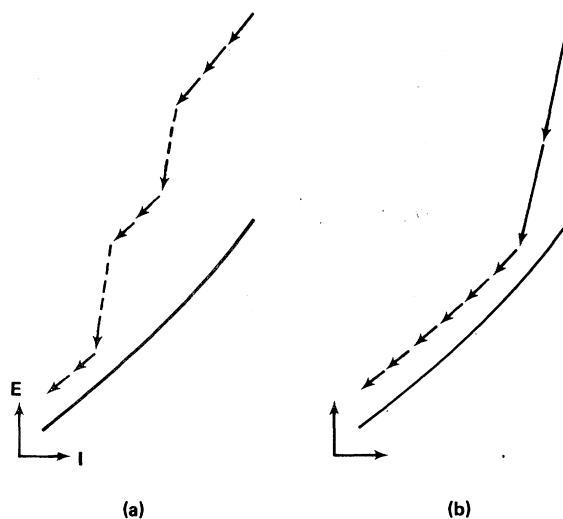


FIG. 7. Different gamma deexcitation patterns which may arise depending on the spreading width  $\Delta E$ . (a) is the scheme of Refs. 4–6 and (b) the original scheme of Ref. 15.

#### ACKNOWLEDGMENTS

This work was supported in part by the National Science Foundation under Contract PHY-79-08395, the Swedish Scientific Research Council, and DOE Contract DE-AC05-76OR00033. The critical comments of A. Bohr, B. R. Mottelson, and K. Neergård were very valuable.

\*Present address: Oak Ridge Associated Universities, Oak Ridge, Tennessee 37830.

<sup>1</sup>J. E. Lynn, *The Theory of Neutron Resonance Reactions* (Clarendon, Oxford, 1968).

<sup>2</sup>*Giant Multipole Resonances*, edited by F. E. Bertrand (Harwood, New York, 1980).

<sup>3</sup>R. M. Diamond and F. S. Stephens, *Annu. Rev. Nucl. Part. Sci.* **30**, 85 (1980).

<sup>4</sup>R. J. Liotta and R. A. Sorensen, *Nucl. Phys.* **A297**, 136 (1978).

<sup>5</sup>M. Wakai and A. Faessler, *Nucl. Phys.* **A307**, 349 (1978).

<sup>6</sup>G. Leander, Y. S. Chen, and B. S. Nilsson, *Phys. Scr.* **24**, 164 (1981).

<sup>7</sup>J. O. Newton, *Phys. Scr.* **24**, 83 (1981).

<sup>8</sup>S. Bjørnholm, *Proceedings of the International Symposi-*

*um on Extreme States in Nuclei*, Dresden, 1980.

<sup>9</sup>A. Bohr and B. R. Mottelson, *Phys. Scr.* **24**, 71 (1981).

<sup>10</sup>P. Ring and H. J. Mang, *Phys. Rev. Lett.* **33**, 1174 (1974).

<sup>11</sup>I. Hamamoto, *Nucl. Phys.* **A271**, 15 (1976).

<sup>12</sup>J. Almberger, I. Hamamoto, and G. Leander, *Nucl. Phys.* **A333**, 184 (1980).

<sup>13</sup>*Statistical Theories of Spectra: Fluctuations*, edited by C. E. Porter (Academic, New York, 1965).

<sup>14</sup>A. Bohr and B. R. Mottelson, *Nuclear Structure* (Benjamin, New York, 1969), Vol. 1, Appendix 2D.

<sup>15</sup>J. O. Newton, F. S. Stephens, R. M. Diamond, W. H. Kelly, and D. Ward, *Nucl. Phys.* **A141**, 631 (1970).

<sup>16</sup>O. Andersen, J. D. Garrett, G. B. Hagemann, B. Herskind, D. L. Hillis, and L. L. Riedinger, *Phys. Rev. Lett.* **43**, 687 (1979).